

TECHNICAL NOTE

Open Access



# On the role of geof foam density on the interface shear behavior of composite geosystems

Mohamed A. Meguid<sup>1\*</sup>  and Muhammad Imran Khan<sup>1,2</sup>

\*Correspondence:  
mohamed.meguid@mcgill.ca  
<sup>1</sup> Civil Engineering  
and Applied Mechanics,  
McGill University, 817  
Sherbrooke St. W., Montreal,  
QC H3A 0C3, Canada  
Full list of author information  
is available at the end of the  
article

## Abstract

Expanded polystyrene (EPS) geof foam has been increasingly used in geotechnical engineering applications to replace conventional backfill material or to reduce earth pressure on retaining and buried structures. In most of these applications, geof foam blocks are installed in direct contact with different construction material (soil, concrete, steel, wood, etc.). This results in a composite system that is subjected to loading in both the normal and shear directions. Therefore, successful analysis and design of these composite structures require a detailed knowledge of interface strength characteristics of geof foam under a combination of normal and shear stresses. In the current research, an attempt has been made to study the interface shear characteristics of geof foam with selected materials, including concrete, wood and steel. Three different geof foam densities namely, 15, 22 and 39 kg/m<sup>3</sup> were used in this study. A series of direct shear tests (DST) was conducted with a shear box of dimension 100 mm × 100 mm × 50 mm under three different normal stresses 18, 36 and 54 kPa. Test results revealed that geof foam density and applied normal stress have significant effects on the vertical compression and interface strength properties (i.e. adhesion and friction angle) of the investigated geosystem. Surface roughness was found to play a significant role in the shear resistance at the contact. Geof foam–concrete interface showed maximum strength as compared to wood and steel materials. Care should be exercised when placing geof foam against steel or wood surfaces as the mobilized friction angle is generally small and sliding may develop depending on the applied normal stress level.

**Keywords:** EPS geof foam, Direct shear tests, Friction angle, Adhesion, Interface shear strength

## Introduction

The use of expanded polystyrene (EPS) geof foam as construction material dates back to the 1960s. Norwegian engineers used EPS geof foam for thermal insulation in road projects constructed in 1965 [1] and large geof foam blocks were used in 1972 as a lightweight fill material in embankments built on soft soils [2]. Since then the use of molded geof foam blocks has been expanded to other geotechnical engineering applications, including slope stabilization [3–7], subbase fill material [8–11], embankments [2, 3, 9, 12–22], earth retaining structures [3, 16], bridge approaches [3, 15, 23–26] and buried pipes [3, 27, 28]. The high compressibility nature of geof foam

material makes it also suitable for applications that require the presence of compressible buffers behind the walls of rigid structures [20, 29–31].

In most of the above applications, EPS geofoam is used in conjunction with other construction materials (e.g. soil, concrete, wood, PVC, steel, geogrid) to form a composite system, which is then exposed to static or dynamic loadings. A schematic that illustrates the use of EPS behind a retaining wall is shown in Fig. 1. Therefore, detailed information of the interface strength is required for successful analysis and design of structures constructed with EPS inclusion. Interface strength is usually determined using the ratio of resisting shear stress to the applied normal stress.

Several researchers investigated the interface shear characteristics of geofoam interacting with different construction materials. A summary of these studies is given below.

Sheeley and Negussey [32] performed a series of modified direct shear tests to study the interface properties of geofoam in contact with geomembrane (smooth or textured) and cast-in-place concrete. Tests were conducted on EPS samples of 18 and 29 kg/m<sup>3</sup> densities under constant normal stress that ranges from 14 to 48 kPa. It was found that both smooth and textured geomembranes offered much less interface friction (both peak and residual) as compared to cast-in-place concrete.

Direct shear tests were conducted by Chrysikos et al. [33] to measure the frictional resistance at the interface between geofoam blocks (densities 15 and 30 kg/m<sup>3</sup>) and other materials (concrete, soils, geomembranes, and geotextiles). The friction coefficients were found to range from 0.27 to 1.2.

Padade and Mandal [34] performed a series of direct shear tests for various geofoam samples interacting with jute geotextile, fly ash, and geogrid. EPS geofoam samples with densities of 15 and 30 kg/m<sup>3</sup> were tested under normal stress range of 25 to 100 kPa. Results showed that the increase in geofoam density resulted in a slight increase in adhesion with no significant change in interface friction angle. For both

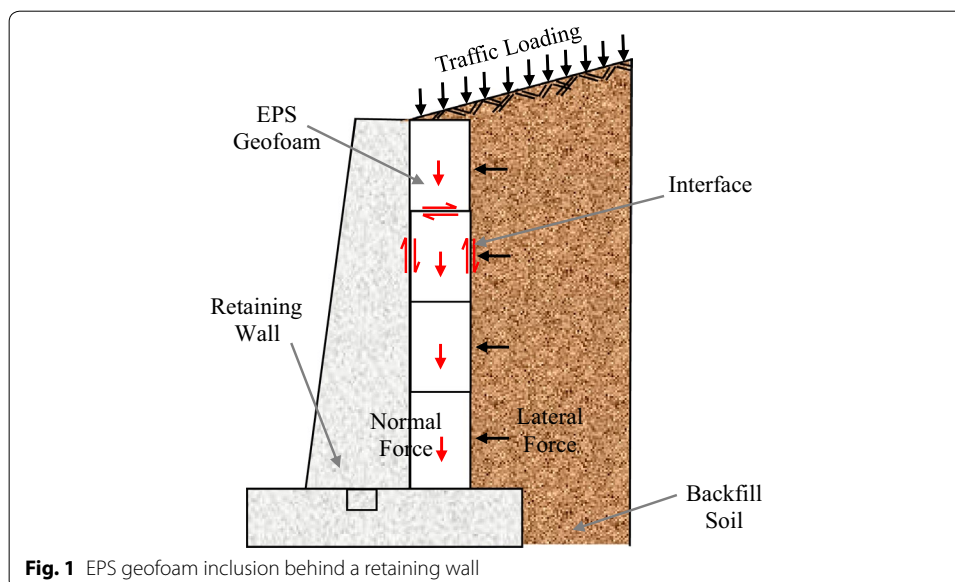


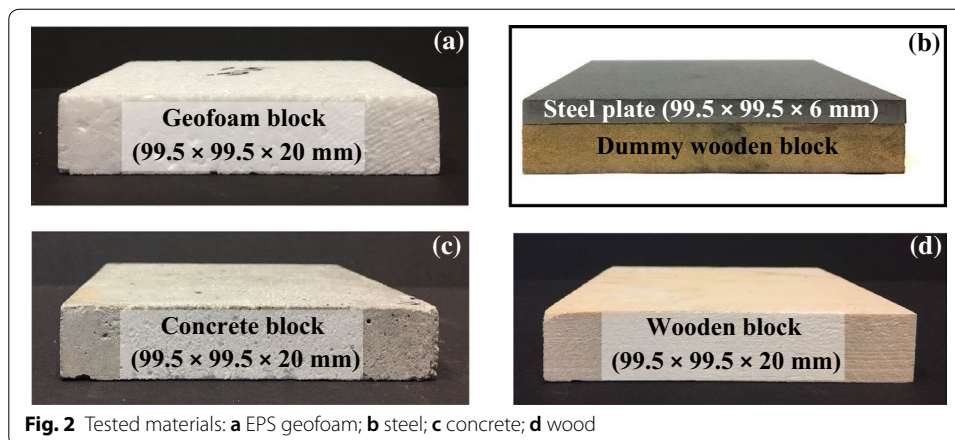
**Table 1 Selected geofoam interface studies**

Reference	Test/ sample size (mm × mm)	Sample density (kg/ m <sup>3</sup> )	Interface	Friction coefficient
Sheeley and Negussey [32]	Direct shear test 100 × 100 × 25	18	Geofoam–cast-in-place concrete	2.36 (peak) 1 (residual)
		–	Geofoam–smooth geomembrane (PVC)	0.7 (peak) 0.4 (residual)
		–	Geofoam–textured geomembrane (PVC)	0.6 (peak) 0.44 (residual)
Chrysikos et al. [33]	Direct shear test	15 and 30	Geofoam–other materials (i.e., soils, geotextiles, geomembranes, pre- cast and cast-in-place concrete)	0.27–1.2
Padade and Mandal [34]	Direct shear test 300 × 300 × 75	15	Geofoam–geotextile	0.17
			Geofoam–geogrid	0.14
			Geofoam–fly ash	0.21
		30	Geofoam–geotextile	0.19
			Geofoam–geogrid	0.12
			Geofoam–fly ash	0.23
AbdelSalam and Azzam [35]	Direct shear test 100 × 100 × 50	20	Geofoam–concrete smooth (dry)	0.49
			Geofoam–concrete smooth (wet)	0.51
		20	Geofoam–concrete rough (dry)	0.96
			Geofoam–concrete rough (wet)	0.48
Khan and Meguid [36]	Direct shear test 100 × 100 × 50	15	Geofoam–PVC block	0.7–1.7
		22	Geofoam–PVC block	0.78–2.0
		35	Geofoam–PVC block	1.2–3.2

geofoam densities, geofoam–geogrid interface showed the least frictional resistance while geofoam–fly ash interface showed the most frictional resistance.

Abdel-Salam and Azzam [35] conducted modified direct shear tests on geofoam–concrete interface under dry and wet conditions. Results indicated that the roughness of the concrete surface has a significant effect on the interface friction coefficient. For dry condition, concrete with rough or textured interface showed much larger frictional resistance over that with a smooth surface. On the contrary, for wet condition, smooth interface developed more frictional resistance.

Khan and Meguid [36] presented experimental results involving geofoam–PVC and geofoam–sand interfaces utilizing EPS samples of 15, 22 and 35 kg/m<sup>3</sup> and a 100 mm × 100 mm direct shear box. To measure the interface coefficient between PVC and geofoam, a PVC block 99.5 × 99.5 × 20 mm was placed in the lower half of the box and then overlain by a geofoam block of the same size. For tests involving geofoam–sand interface, silica sand was compacted in layers in the lower half of the box to reach a density of 1.6 g/cm<sup>3</sup>. Tests were performed under a normal stress that ranged from 18 to 54 kPa. Results showed that geofoam–sand interface developed frictional resistance that is much larger than that measured for the geofoam–PVC interface. A summary of some of the available interface friction coefficients is given in Table 1.



### Scope and objectives

Although the above studies covered important aspects related to the interface strength of geofoam interacting with various construction material, there is a need for additional investigations to understand how geofoam density affects the interface strength for a range of materials. The aim of this study is, therefore, to evaluate the role of EPS density on the interface shear strength of three different materials, namely, concrete, wood and steel. Details of “[Experimental program](#)” are given in the subsequent section.

### Experimental program

A series of direct shear tests were performed to evaluate the interface shear properties of different EPS geofoam blocks placed over a given construction material. A total of nine experiments were performed for each of the three investigated materials (concrete, wood, and steel) such that the test is repeated three times for each geofoam density (15, 22, and 39 kg/m<sup>3</sup>). “[Material properties](#)” and “[Test procedure](#)” are given below.

### Material properties

The materials used in this investigation include EPS geofoam, concrete, wood and steel as depicted in Fig. 2. Three different sets of geofoam samples with densities of 15 kg/m<sup>3</sup> (EPS15), 22 kg/m<sup>3</sup> (EPS22) and 39 kg/m<sup>3</sup> (EPS39) were examined. These material densities cover a wide range of EPS geofoam used in geotechnical projects [37]. Before commencing the interface tests, uniaxial compressive strength tests were performed on the EPS samples as per ASTM D1621-10 (2010) specifications. The uniaxial compression curves (presented in Fig. 3) are characterized by a linear increase in response up to about 1% strain (calculated as the ratio of sample compression to the original sample height). This is followed by an increase at a slower rate up to the maximum applied stress. The uniaxial compressive strength properties are summarized in Table 2. For EPS15, the uniaxial compressive strength at 1% strain was found to be 50 kPa which increased to 80 kPa at 5% strain and reached 90 kPa at 10% strain. These strength values were almost doubled for EPS22 where the strength values at 1% and 5% strains were found to be 63 kPa and 125 kPa, respectively.

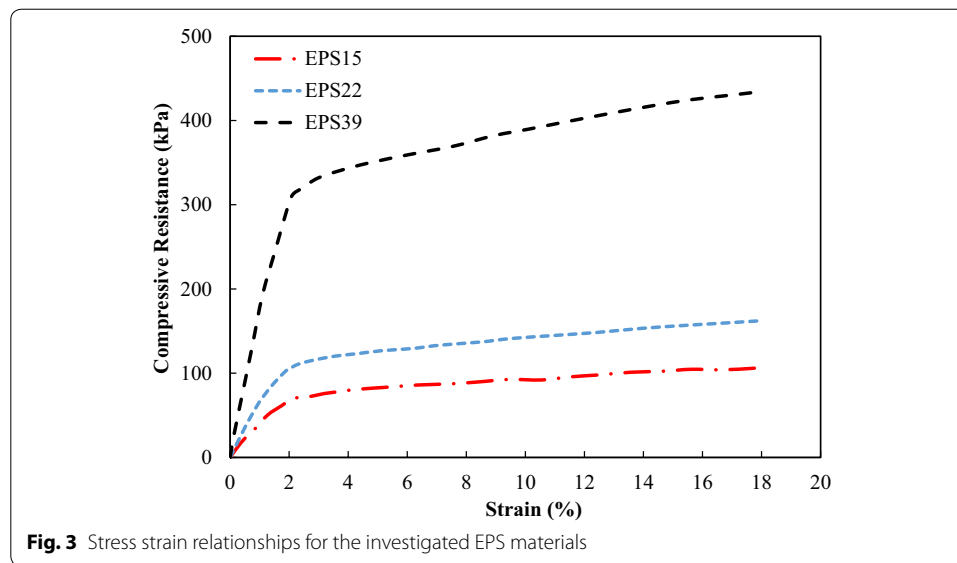


**Table 2** Mechanical properties of EPS geofoam-ASTM D6817 [40]

Type	EPS15	EPS22	EPS39
Density (kg/m <sup>3</sup> )	14.4	21.6	38.4
Compressive resistance (kPa) at 1%	50	63	190
Compressive resistance (kPa) at 5%	80	125	350
Compressive resistance (kPa) at 10%	90	140	385

The steel, concrete and wood samples were cut accurately to fit into the lower part of the direct shear box. Plain concrete samples were prepared using fine and coarse granite with a water-cement ratio of 0.65 which has a slump of 228 mm. Visual inspection of samples revealed that the concrete surface was rough while pine wood and steel were characterized by a relatively smooth surface of different texture. Properties of all the three materials as obtained from the manufacturer are given in Table 3.

### Test procedure

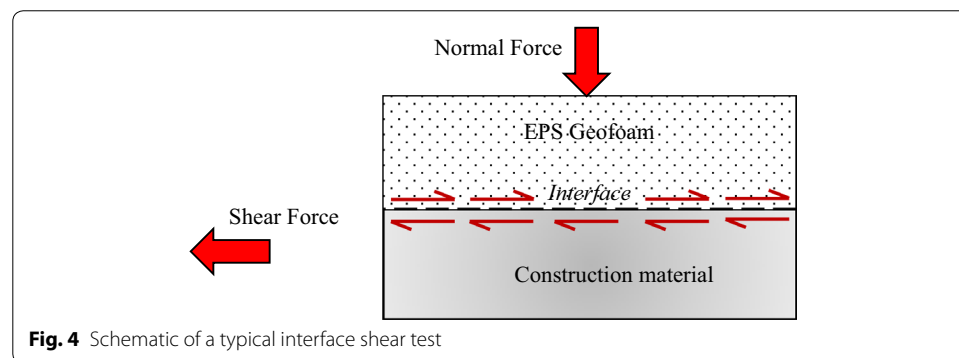
Interface direct shear tests were performed throughout this study following ASTM D5321-17 [38]. A direct shear box of dimensions 100 mm × 100 mm × 50 mm was used throughout this study. For each interface test, a geofoam sample was placed in the upper part of the box while the other block of interacting material was placed in the lower part of the box as shown in Fig. 4. This arrangement ensures full contact between the two samples during the test. It also reduces the chances of tilting that may develop if the lower sample compresses non-uniformly. Due to the heavy weight of the steel block, a thin 6-mm steel plate was used with 14 mm dummy wooden block (see Fig. 2b). This allowed for the weight of the box to be easily managed.

During the test, a horizontal displacement was applied to the lower half of the box at a rate of 0.9 mm/min while the upper half was fixed. Tests were conducted under normal

**Table 3 Properties of material used**

Properties of concrete	
w/c ratio	0.65
Cement (c)	335 kg/m <sup>3</sup>
Water (w)	218 kg/m <sup>3</sup>
Coarse granite	1060 kg/m <sup>3</sup>
Fine granite	680 kg/m <sup>3</sup>
Concrete density	2293 kg/m <sup>3</sup>
Slump	228 mm
Properties of steel <sup>a</sup>	
Density	8142 kg/m <sup>3</sup>
Yield strength	60,000 psi (413.685 MPa)
Tensile strength	95,000 psi (655 MPa)
Elastic modulus	27,557–30,458 ksi (190–210 GPa)
Poisson's ratio	0.27–0.30
Hardness (rockwell)	B 90 (medium)
Properties of pine wood <sup>a</sup>	
Density	375 kg/m <sup>3</sup>
Tensile strength, ultimate	305 psi (2103 Pa)
Modulus of rupture	8.56 ksi (59 MPa)
Flexural yield strength	6000 psi (413.69 MPa)
Flexural modulus	1200–1240 ksi (8274–8550 MPa)
Compressive yield strength	508 psi (3503 kPa)
Shear strength	899 psi (6198 kPa)

<sup>a</sup> Provided by the manufacturer



stresses of 18, 36 and 54 kPa. Vertical and horizontal displacements were measured using linear variable differential transformers (LVDTs) and the shear force was measured using a load cell. Tests were terminated when the shear force started to decrease or when the maximum displacement allowed by the direct shear box (i.e. 10 mm) was reached. According to ASTM D3080-11 [39], if no peak behavior is observed during the test, peak shear stress may be considered to develop at 10% horizontal strain. Adhesion and interface friction angles were determined from the results of the direct shear tests for different geof foam densities.

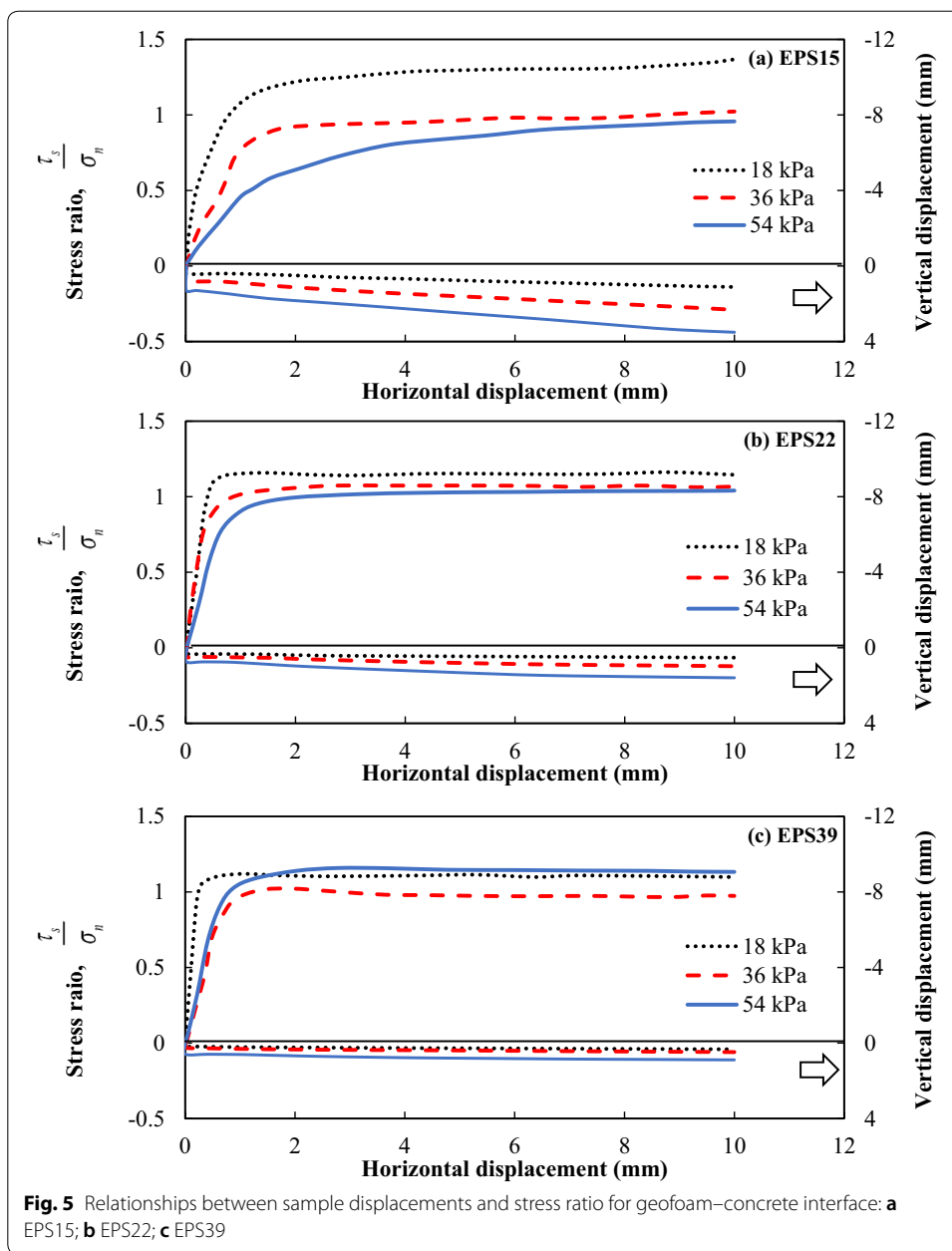
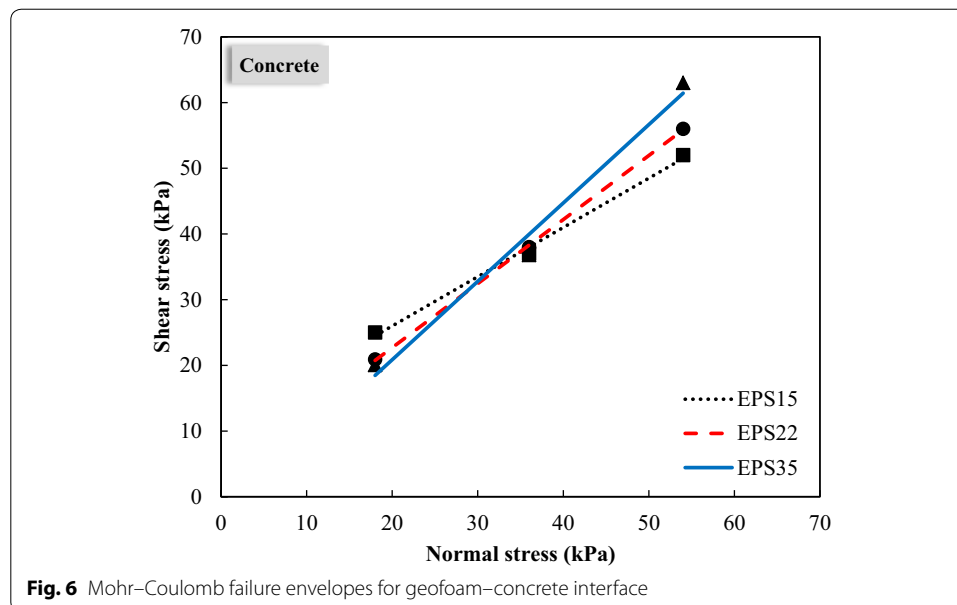


**Fig. 5** Relationships between sample displacements and stress ratio for geofoam–concrete interface: **a** EPS15; **b** EPS22; **c** EPS39

### Results and discussion

The results of the performed tests are presented in this section for the three investigated materials (concrete, steel and wood). The role of geofoam density in each case is highlighted. Stress–displacement relationships are presented using the normalized stress ratio that represents the ratio between shear and normal stresses as measured in the experiments.



### Interface strength properties

#### *Geofoam-concrete interface*

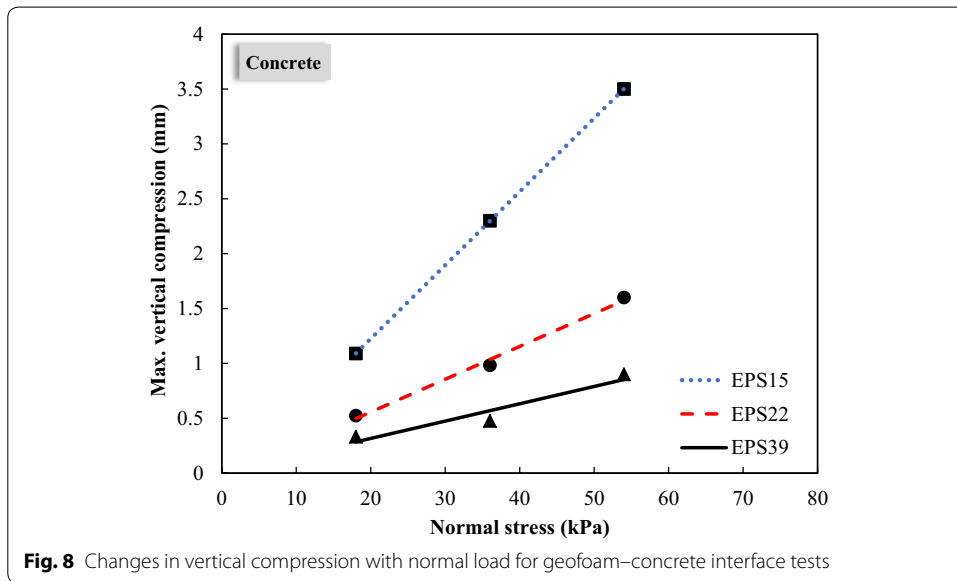
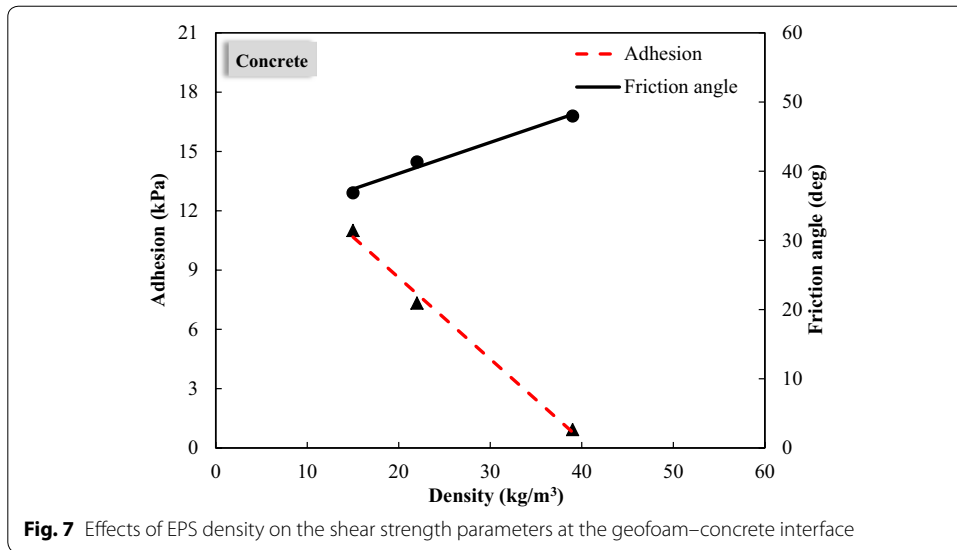
The relationship between shear stress ratio and the sample displacements are presented in Fig. 5 for the three investigated geofoam densities. The applied normal stresses ranged between 18 and 54 kPa. For EPS15 (Fig. 5a), samples generally showed hardening behavior following an initial linear response. The shear stress ratio was found to decrease with the increase in applied normal stress. Figure 5a also shows that the increase in normal stresses is directly related to the increase in the measured vertical displacement of the sample. The maximum vertical displacements at the end of the tests were found to be 3.8 mm, 2.2 mm, and 1 mm for applied normal stress of 18, 36 and 54 kPa, respectively.

For EPS22 and EPS39 (Fig. 5b, c), the behavior is characterized by stiffer response as compared to EPS15. This is evident from the small displacement level required to reach the maximum stress ratio. The response reached a plateau at a horizontal displacement of about 2 mm for the investigated range of normal stresses.

The vertical displacements (compression) of the EPS22 and EPS39 samples were found to reach maximum values of 1.8 mm and 0.9 mm, respectively. These values are consistent with the increase in geofoam density under the same level of normal stress.

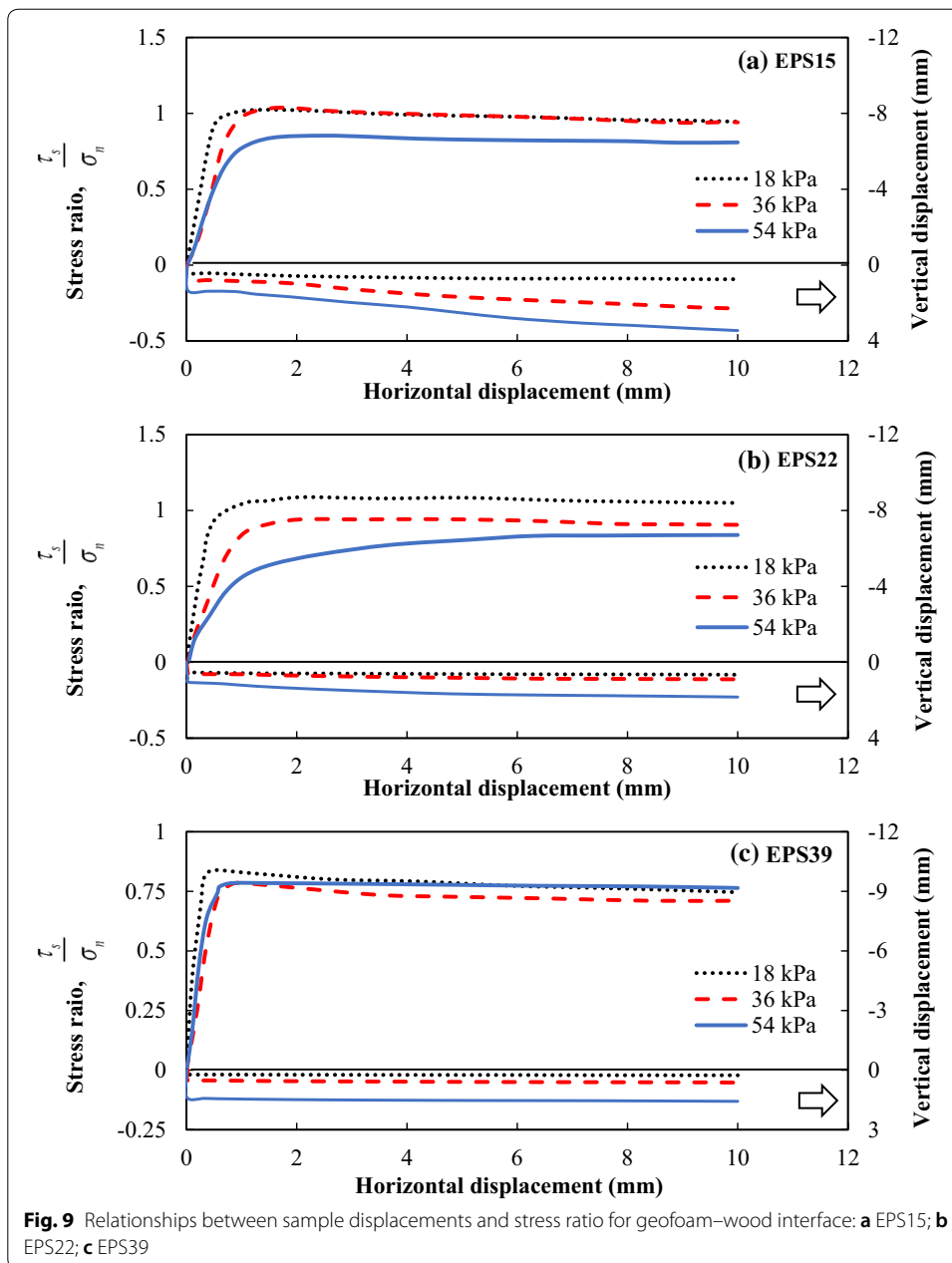
The failure envelopes developing at the geofoam-concrete interface for the three investigated EPS samples are presented in Fig. 6. Interface friction angles and the corresponding adhesion values along the contact surface are determined using the slopes and intercepts of the failure envelope. It was found that friction angles generally increased with the increase in geofoam density. Adhesion, on the other hand, was found to decrease with the increase in geofoam density. This could be attributed to the fact that under low applied normal stress, less interaction develops between the high-density geofoam (EPS22 and EPS39) and the concrete surface as compared to EPS15. The effect of geofoam density on the interface shear strength parameters is further illustrated in Fig. 7 by plotting the material density on the horizontal axis and the shear strength parameters





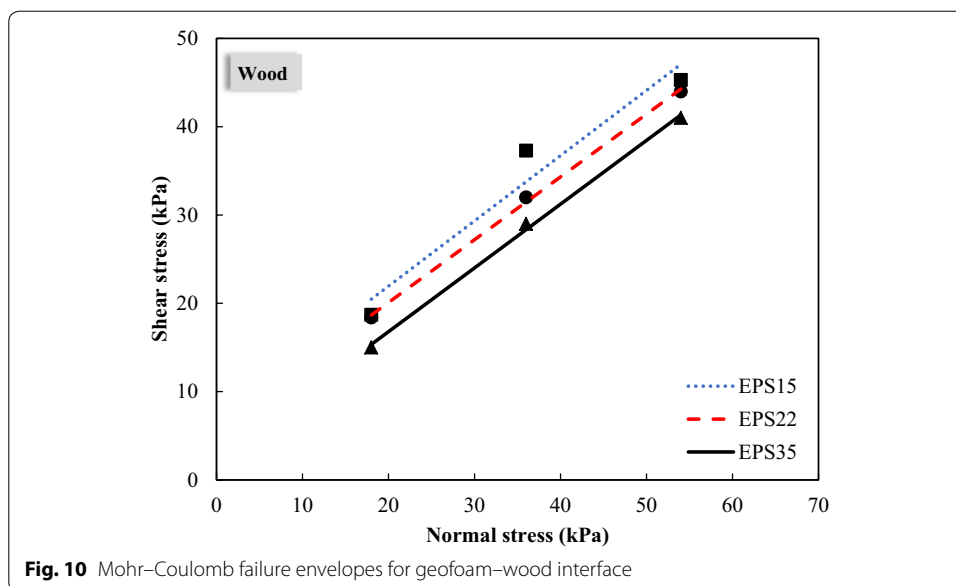
on the vertical axes. It is evident that the interface friction angle increases at a slow rate from 37° to 48° as the EPS density increased from 15 to 39 kg/m<sup>3</sup>, whereas the adhesion along the contact surface rapidly decreased from about 11 to 1 kPa.

Figure 8 shows the effect of geofoam density on the maximum vertical compression of the samples as measured in the experiments. The results show that sample compression reached 3.5 mm (about 17% of the sample height) for EPS15 under normal stress of 54 kPa. The compression significantly decreased to 1.6 mm for EPS22 and 0.9 mm for EPS39. This response is consistent with the increase in material stiffness associated with the increase in density.



**Geofoam–wood interface**

For geofoam–wood interface tests, stress ratios were plotted against sample displacements as depicted in Fig. 9. Samples were tested under applied normal stresses that range from 18 to 54 kPa. For EPS15 and EPS22 (Fig. 9a, b), initially, stress ratio increased linearly with the increase in sample displacement and then reached the maximum stress ratio at applied displacement that depends on the stress level. For EPS39, the maximum stress ratio reached about 0.75 with a maximum horizontal displacement of around 10 mm. EPS15 and EPS22 were found to reach maximum vertical displacement of 3.8 mm and 1.8 mm, respectively under normal stress of 54 kPa.



For EPS39, a slightly stiffer response was observed (Fig. 9c) such that maximum stress ratios corresponded to smaller displacements as compared to the other geofoam cases.

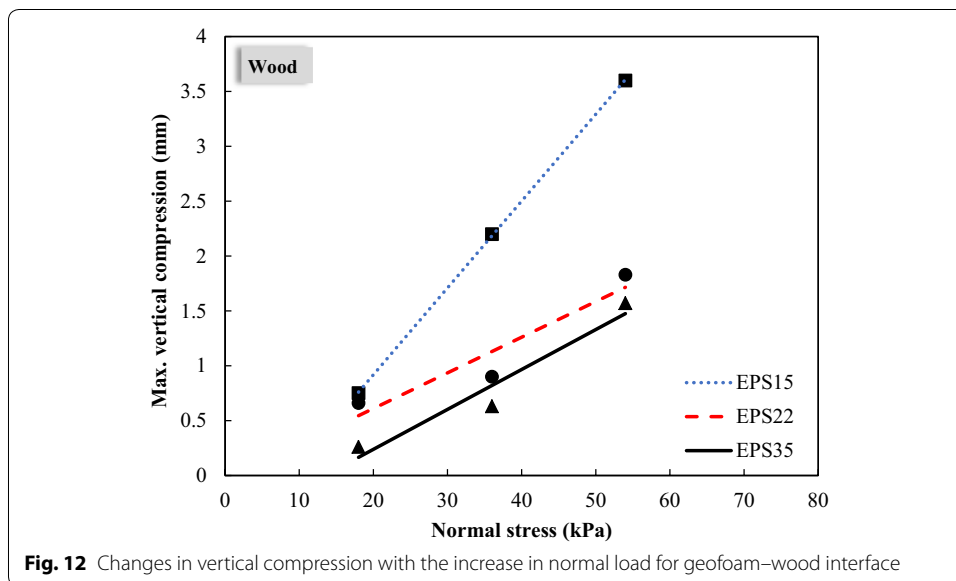
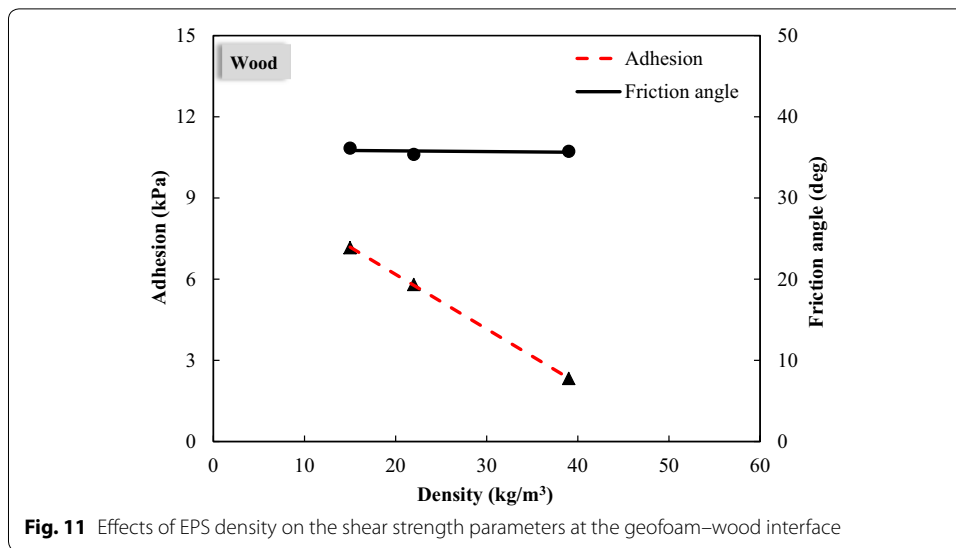
Vertical displacements measured showed trends that are consistent with those observed in the previous tests where sample compression decreased with the increase in geofoam density.

Mohr-Coulomb failure envelopes were plotted and interface strength parameters were calculated for all geofoam-wood interface tests as shown in Fig. 10. Failure envelopes were generally parallel with upward slope. Interface shear strengths values were found to increase with the increase in normal stress and decreases with the increase in geofoam density. This may be attributed to the fact that low density geofoam (EPS15) develops more interaction with the wood grains as compared to higher density geofoam (EPS39) under the same applied normal stress. As the geofoam density increased from 15 to 39 kg/m<sup>3</sup>, adhesion values decreased from 7.6 to 2.33 kPa whereas the angles of interface friction remained almost unchanged as shown in Fig. 11.

Figure 12 shows the relationship between the maximum vertical displacements and the applied normal stress for the three investigated geofoam densities. Results show that vertical compression of geofoam is directly related to applied normal stress and inversely related to geofoam density. EPS15 showed maximum compression of 3.6 mm (18% of the sample height) while EPS39 showed maximum compression of 1.6 mm (8% of the sample height). The rate of increase in sample compression was more rapid for EPS15 as compared to the two other densities.

**Geofoam-steel interface**

The relationships between the stress ratio and measured horizontal displacements for the case of geofoam-steel interaction are shown in Fig. 13a-c for EPS15, EPS22 and



EPS39, respectively. EPS15 showed insignificant hardening behavior (Fig. 13a) with soft response at small strains compared to EPS22 and EPS39 (Fig. 13b, c). The maximum stress ratios reached 0.8, 0.65, 0.56 at displacements of 1 mm, 0.45 mm, and 0.4 mm for EPS15, EPS22 and EPS39, respectively. In addition, vertical displacements measured during the shear tests showed trends that are consistent with the geofoam density. EPS15, EPS22 and EPS39 experienced maximum compression values of 3.2 mm, 1.1 mm and 0.7 mm, respectively, under an applied normal stress of 54 kPa.

For all geofoam–steel interface tests, linear Mohr–Coulomb failure envelopes were plotted in Fig. 14. It was found that for a particular value of normal stress, higher density geofoam samples showed lower interface strength as compared to lower density geofoam. This is attributed to the fact that low density geofoam interacts better with the contacting material as compared to high density geofoam. This observation is also

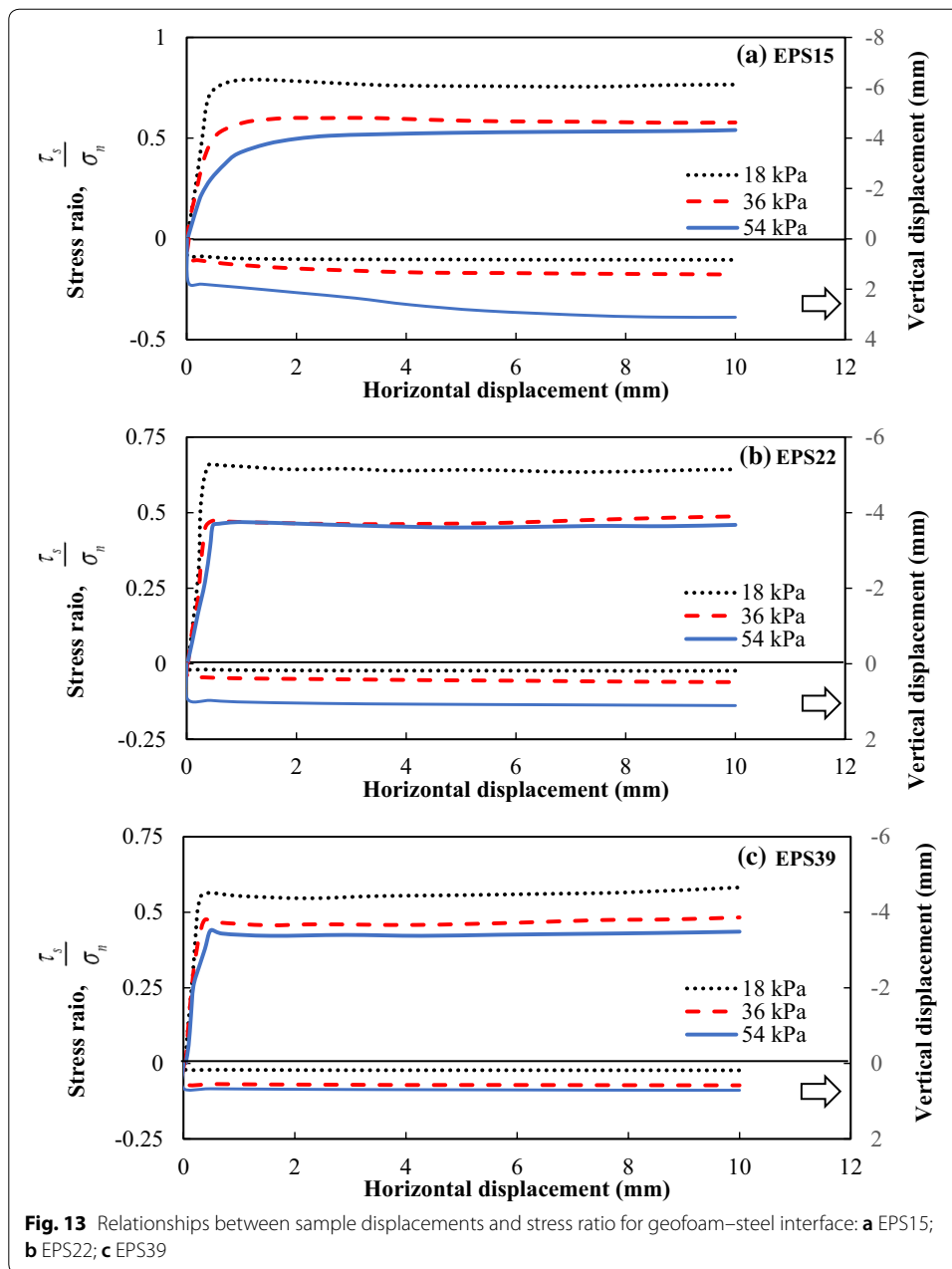


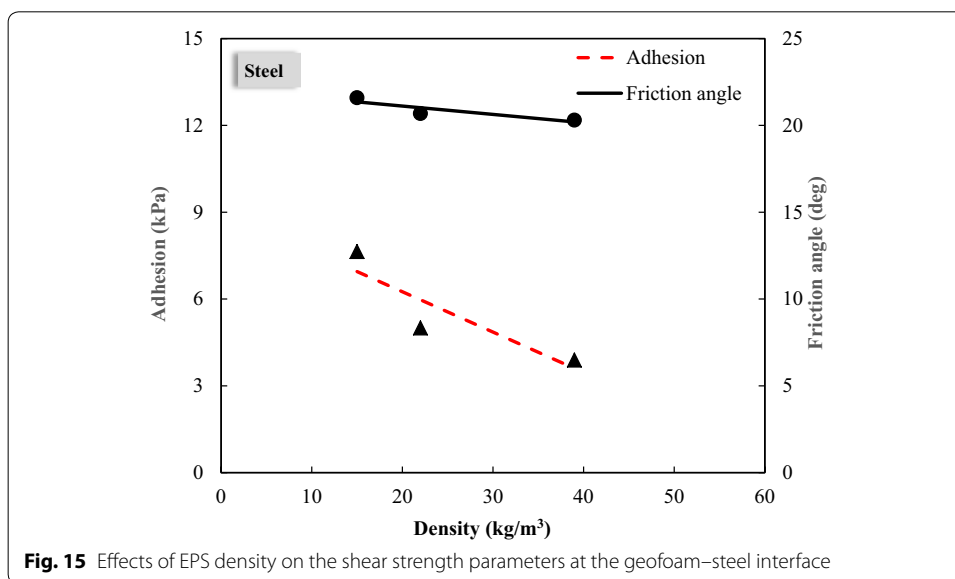
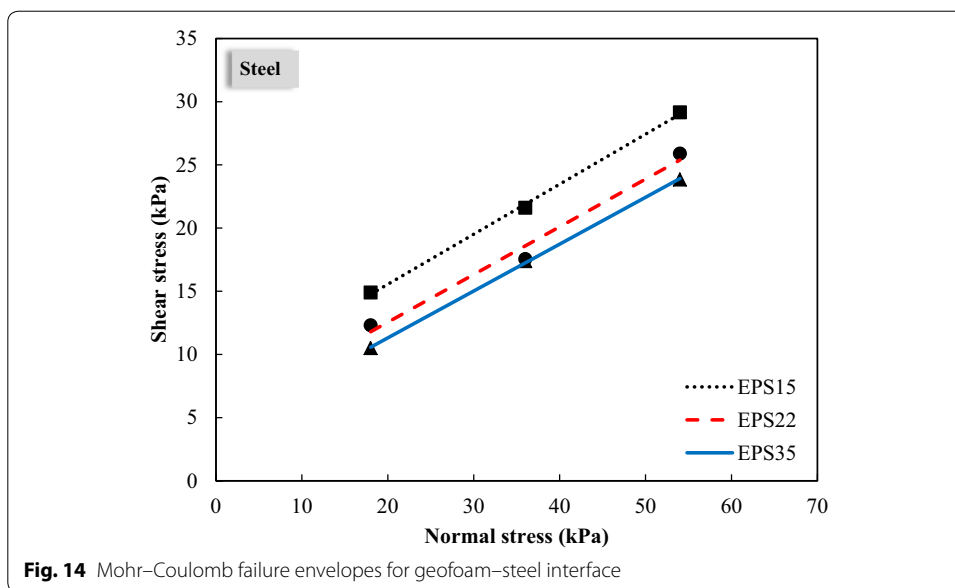
**Fig. 13** Relationships between sample displacements and stress ratio for geofoam–steel interface: **a** EPS15; **b** EPS22; **c** EPS39

confirmed by the decrease in adhesion from 7.6 to 3.9 kPa and decrease in angle of interface friction from 21.6° to 20.3° as shown in Fig. 15.

Maximum compression is plotted in Fig. 16 for the range of applied normal stress. Trends are found to be consistent with previous test results where the rate of compression was rapid for EPS15 compared to the rest of the samples.

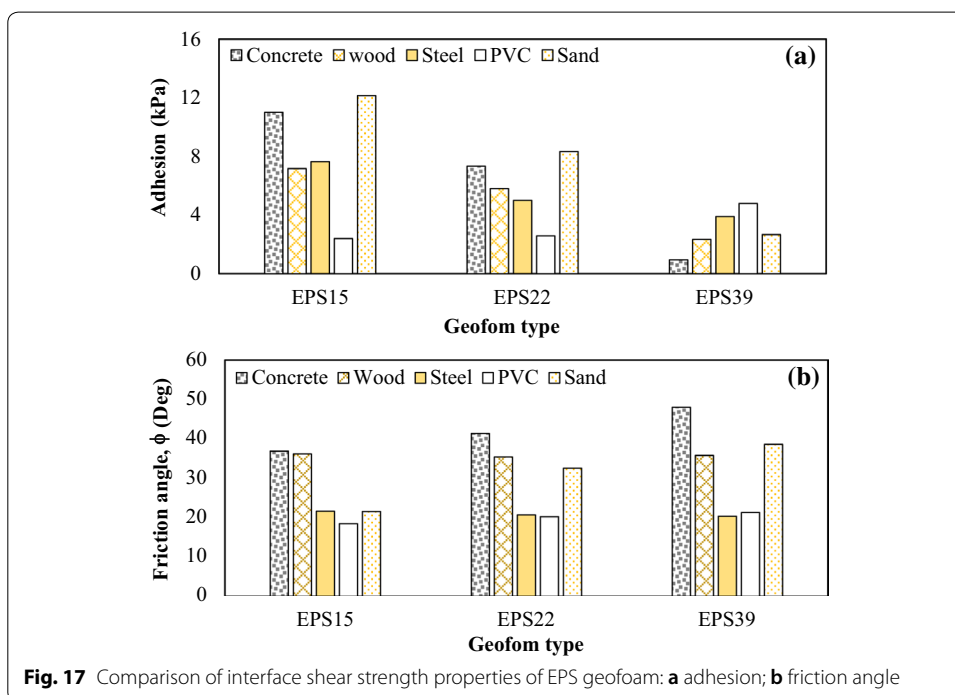
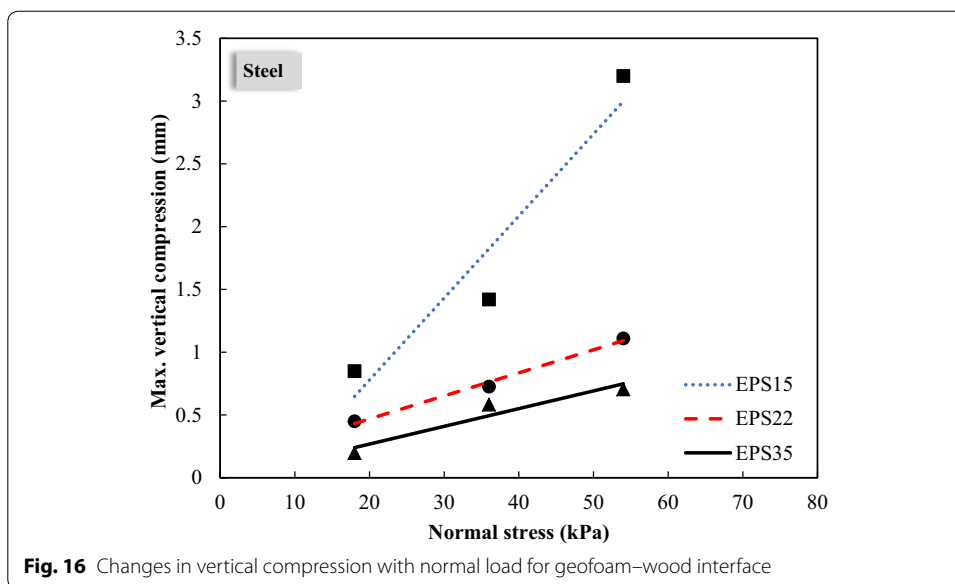
**Practical significance**

For comparison purpose, the results of this study are combined with those reported by Khan and Meguid [36] for cases involving geofoam–sand and geofoam–PVC interaction as summarized in Fig. 17. It should be noted that the density of EPS39 used



in this study is slightly different from EPS35 used previously by Khan and Meguid [36]. This is attributed to the changes made during the manufacturing process and therefore, the results presented for EPS39 for sand and PVC materials are considered approximate.

For all investigated materials, adhesion at the interface generally decrease with the increase in geofoam density (Fig. 17a) except for PVC where the adhesion was relatively small due to the low surface roughness. EP15 and EPS22 seem to interact better with construction material of rough surfaces particularly sand and concrete. Under the same normal load, EPS39 did not allow enough surface interaction resulting in



smaller adhesion for all studies materials. As far as the friction angle component of the interface strength, concrete, wood, and sand presented higher surface friction that increased with the increase in EPS density. This was not the case for steel and PVC as the friction angle did not significantly change and was about half of that of the concrete material. A summary of the measured test results and the average friction coefficient values for each material is provided in Table 4.

The practical significance of these results is that EPS density plays a role in the interface shear strength properties of a composite system. The reported values in this

**Table 4 Summary of experimental results**

Test/sample size (mm × mm)	Sample density (kg/ m <sup>3</sup> )	Interface	Coefficient of friction	
			Measured	Average
Direct shear test 100 × 100 × 50	15	Geofoam–concrete	0.96–1.39	1.2
	22		1.04–1.33	1.1
	39		1.17–1.28	1.2
Direct shear test 100 × 100 × 50	15	Geofoam–wood	0.84–1.04	0.95
	22		0.81–1.02	0.92
	39		0.76–0.83	0.80
Direct shear test 100 × 100 × 50	15	Geofoam–steel	0.54–0.79	0.67
	22		0.47–0.66	0.56
	39		0.44–0.58	0.50

study may be used to estimate the expected shear resistance when designing a geotechnical structure with EPS geofoam inclusion that may experience movement along the interface.

## Conclusions

In this study, 27 direct shear tests were performed to investigate the behavior of geofoam in contact with different construction materials. Tests were conducted using three geofoam densities interacting with three different construction materials, namely, concrete, wood and steel. The following conclusions have been drawn from this experimental study.

1. When EPS geofoam blocks are subjected to a combination of normal and shear stresses, geofoam density and applied normal stress play an important role on the shear resistance at the interface.
2. Geofoam blocks in contact with concrete, wood and steel showed a decreasing trend in adhesion as the geofoam density increased from 15 to 39 kg/m<sup>3</sup>. However, the interface friction angle was found to increase for the case of concrete compared to other materials.
3. Vertical compression of EPS geofoam showed trends consistent with the geofoam density for all investigated materials. Compression values are directly related to applied normal stress and inversely related to geofoam density.
4. Using rough surface concrete is recommended for projects involving EPS geofoam blocks in direct contact with the concrete and backfilled with sand material as the increase in interface friction coefficient on both sides of the geofoam blocks will result in an increase in the shear resistance of the composite system.

## Acknowledgements

The present study is jointly funded by McGill University and the University of Engineering and Technology, Lahore, Pakistan. The assistance of Mr. John Bartczak and the in-kind support from Plasti-Fab Inc. are highly appreciated. This study was funded by Natural Sciences and Engineering Research Council of Canada (RGPIN-2016-05263).

## Authors' contributions

MIK carried out the experimental work under the supervision of MAM. Both authors read and approved the final manuscript.



**Competing interests**

The authors declare that they have no competing interests.

**Author details**

<sup>1</sup> Civil Engineering and Applied Mechanics, McGill University, 817 Sherbrooke St. W., Montreal, QC H3A 0C3, Canada.

<sup>2</sup> Civil Engineering Department, University of Engineering and Technology, Lahore, Pakistan.

Received: 7 October 2018 Accepted: 28 May 2019

Published online: 30 May 2019

**References**

1. Aaboe R (2000) Evidence of EPS long term performance and durability as a light weight fill. Vegteknisk avdeling
2. Frydenlund T (1991) Expanded polystyrene: a lighter way across soft ground, vol 1502. ICON Group International, San Diego
3. Elragi AF (2000) Selected engineering properties and applications of EPS geofoam. ProQuest Dissertations and Theses
4. Jutkofsky W, Sung J, Negussey D (2000) Stabilization of embankment slope with geofoam. Transport Res Record 1736:94–102
5. Sheeley M (2000) Slope stabilization utilizing geofoam. Master's Thesis, Syracuse University, New York
6. Srirajan S (2001) Recycled content and creep performance of EPS geofoam in slope stabilization
7. Negussey D (2002) Slope stabilization with geofoam. Report to FHWA and the EPS industry. Geofoam Research Center, Syracuse University, New York
8. Stark TD, Arellano D, Horvath JS, Leshchinsky D (2004) Geofoam applications in the design and construction of highway embankments. NCHRP Web Document 65:24–31
9. Duskov M (1991) Use of expanded polystyrene (EPS) in flexible pavements on poor subgrades. In: Proceedings of the international conference on geotechnical engineering for coastal development, pp 783–788
10. Duskov M (1997) Measurements on a flexible pavement structure with an EPS geofoam sub-base. Geotext Geomembr 15(1):5–27. [https://doi.org/10.1016/S0266-1144\(97\)00004-6](https://doi.org/10.1016/S0266-1144(97)00004-6)
11. Riad HL, Ricci AL, Osborn PW, Horvath JS (2003) Expanded polystyrene (EPS) geofoam for road embankments and other lightweight fills in urban environments. In: Soil and rock America, 12th Pan-American conference on soil mechanics and geotechnical engineering and 39th US rock mechanics symposium
12. Refsdal G (1985) Plastic foam in road embankments: future trends for EPS use. Internal report. Norwegian Road Research Laboratory, Oslo
13. Aaboe R (1987) 13 years of experience with expanded polystyrene as a lightweight fill material in road embankments. Norwegian Road Research Laboratory Publication 61:21–27
14. Magnan J, Serratrice J (1989) Mechanical properties of expanded polystyrene for applications in road embankment. Bull Liaison LCPC 164:25–31
15. Williams D, Snowdon R (1990) A47 Great Yarmouth Western Bypass: performance during the first three years, No. 11
16. Frydenlund T, Aaboe R (1996) Expanded polystyrene—the light solution. In: Proceedings of international symposium on EPS (expanded poly-styrol) construction method (EPS Tokyo'96)
17. Van Dorp T (1996) Building on EPS geofoam in the 'low-lands'. Experiences in the Netherlands. In: Proceedings of international symposium on EPS (Expanded Poly-Styrol) construction method (EPS Tokyo'96)
18. Zou Y, Leo C, Small J (2000) Behaviour of EPS geofoam as flexible pavement subgrade material in model tests. Geosynth Int 7(1):1–22
19. Negussey D, Stuedlein A, Bartlett S, Farnsworth C (2001) Performance of a geofoam embankment at 100 South, I-15 reconstruction project, Salt Lake City, Utah. In: Proceedings on 3rd international conference on EPS Geofoam
20. Zarnani S, Bathurst R (2007) Experimental investigation of EPS geofoam seismic buffers using shaking table tests. Geosynth Int 14(3):165–177
21. Farnsworth C, Bartlett SF, Negussey D, Stuedlein A (2008) Rapid construction and settlement behavior of embankment systems on soft foundation soils. J Geotech Geo-Environ Eng 134(3):289–301
22. Newman MP, Bartlett S, Lawton E (2009) Numerical modeling of geofoam embankments. J Geotech Geo-Environ Eng 136(2):290–298
23. Skuggedal H, Aaboe R (1991) Temporary overpass bridge founded on expanded polystyrene. In: Proceedings of the 1st European conference on soil mechanics and foundation engineering, pp 559–561
24. McDonald P, Brown P (1993) Ultra lightweight polystyrene for bridge approach fill. In: Proceedings of the 11th Southeast Asian geotechnical conference, Singapore, pp 664–668
25. Bang S (1995) Experimental and analytical study of expanded polystyrene blocks in highway application. In: Proceedings of international seminar on the application of EPS for embankment construction, Korea Institute of Construction Technology (KICT), Seoul, Korea, pp 105–133
26. Abu-Hejleh N, Zornberg JG, Elias V, Watcharamonthein J (2003) Design assessment of the founders/meadows GRS abutment structure. In: Proceeding on 82nd annual TRB meeting
27. Meguid M, Hussein M, Ahmed M, Omeman Z, Whalen J (2017) Investigation of soil–geosynthetic–structure interaction associated with induced trench installation. Geotext Geomembr 45(4):320–330
28. Meguid M, Ahmed M, Hussein M, Omeman Z (2017) Earth pressure distribution on a rigid box covered with u-shaped geofoam wrap. Int J Geosynth Ground Eng 3(2):11
29. Horvath J (1997) The compressible inclusion function of EPS geofoam. Geotext Geomembr 15(1):77–120
30. Bathurst RJ, Keshavarz A, Zarnani S, Take WA (2007) A simple displacement model for response analysis of EPS geofoam seismic buffers. Soil Dyn Earthq Eng 27(4):344–353
31. Ossa A, Romo M (2011) Dynamic characterization of EPS geofoam. Geotext Geomembr 29(1):40–50

32. Sheeley M, Negussey D (2000) An investigation of geofoam interface strength behavior. *Geotech Special Publ* 301:292–303. [https://doi.org/10.1061/40552\(301\)23](https://doi.org/10.1061/40552(301)23)
33. Chryssikos D, Atmatzidis D, Missirlis E (2006) EPS geofoam surface shear resistance. 8thIGS Yokohama, Japan, pp 1651–1654
34. Padade A, Mandal J (2014) Interface strength behavior of expanded polystyrene EPS geofoam. *Int J Geotech Eng* 8(1):66–71
35. Abdel Salam S, Azzam S (2016) Reduction of lateral pressures on retaining walls using geofoam inclusion. *Geosynth Int* 23(6):395–407
36. Khan M, Meguid M (2018) Experimental investigation of the shear behavior of EPS geofoam. *Int J Geosynth Ground Eng* 4:12
37. Xiao M (2015) *Geotechnical engineering design*. Wiley, New York
38. ASTM D5321/D5321M-17 (2017) Standard test method for determining the shear strength of soil-geosynthetic and geosynthetic-geosynthetic interfaces by direct shear. ASTM International, West Conshohocken. <http://www.astm.org>
39. ASTM D3080/D3080M-11 (2011) Standard test method for direct shear test of soils under consolidated drained conditions. ASTM International, West Conshohocken. <http://www.astm.org>
40. ASTM D6817/D6817M-17 (2017) Standard specification for rigid cellular polystyrene geofoam. ASTM International, West Conshohocken. <http://www.astm.org>

### **Publisher's Note**

Springer Nature remains neutral with regard to jurisdictional claims in published maps and institutional affiliations.

**Submit your manuscript to a SpringerOpen<sup>®</sup> journal and benefit from:**

- ▶ Convenient online submission
- ▶ Rigorous peer review
- ▶ Open access: articles freely available online
- ▶ High visibility within the field
- ▶ Retaining the copyright to your article

---

Submit your next manuscript at ▶ [springeropen.com](http://springeropen.com)

---